LA-6859-MS
Informal Report

C.3

The Polymorphic Detonation

Wildon Fickett

**los alamos
scientific laboratory
of the University of California**
LOS ALAMOS, NEW MEXICO 87545

An Affirmative Action/Equal Opportunity Employer

Printed in the United States of America. Available from
National Technical Information Service
U.S. Department of Commerce
5285 Port Royal Road
Springfield, VA 22161
Price: Printed Copy $3.50 Microfiche $3.00

NOMENCLATURE

Part A

C - constant-volume heat capacity
D - detonation velocity
e - internal energy
k - volume-increase parameter
p - pressure
$q = \Delta v_0$, volume change at p_0
r - reaction rate
t - time
u - particle velocity
v - volume $(= 1/\rho)$
x - position
λ - degree of transformation
ρ - density $(= 1/v)$

● Mixture quantities

$\bar{v} = (1 - \lambda)\, v_1 + \lambda v_2$
$\Delta v = v_2 - v_1$

● Sub- and superscripts

e - equilibrium
i - phase (i = 1 or 2)
j - CJ detonation final state
r - CJ deflagration final state
o - initial state
* - transition value

● Terms

CJ - Chapman-Jouguet
EOS - equation of state
"fire" - reaction zone
"reaction" - process of phase transformation

● Units

All extensive quantities are specific (per unit mass). Units are any consistent set.

Part B

ϵ - viscosity parameter ($\epsilon = 0$ is the inviscid limit)
k - $\hat{v}_2/\hat{v}_1$
m - mass flux
ν - viscosity coefficient
π - viscous pressure $\nu\, u_x$
R — Rayleigh function $(p - p_0)/m^2 - (v_0 - v)$
z - rate multiplier
EOS - $p = \hat{p}\hat{v}_1^2\, (1 + q\lambda)^2/v^2$; $q = k - 1$
sub zero - initial state
super caret - EOS parameter (denoted by sub zero in Part B)

THE POLYMORPHIC DETONATION

by

Wildon Fickett

ABSTRACT

The steady detonation whose driving force is the volume change in a polymorphic phase transition is discussed. The problem is simplified by using an idealized equation of state for which the pressure depends on the density and composition, but not on the internal energy. Both the inviscid and viscid cases are treated.

The phase transition may be represented schematically as

$$A_1 \rightleftarrows A_2$$

$$\lambda = 0_1 \qquad 1 \quad ,$$

with A_2 the lower density phase and λ the transformation progress variable (mass fraction of phase 2). The initial state for the detonation is pure phase 1 ($\lambda = 0$) in a metastable state well below the transition pressure. Possible examples are stishovite-quartz, diamond-carbon, and water-ice, with initial states metastable stishovite, metastable diamond, and supercooled water, respectively.

Different wave structures are found, including double waves in which a decoupled transformation zone moves more slowly than the shock.

PART A
INVISCID CASE

We treat an idealized system in which thermal effects are largely ignored. We assume local thermodynamic equilibrium for all variables other than the composition and neglect interfacial effects at the physical boundary between the two phases. Thus the temperature and pressure of the two phases are always the same, the transformation of one phase to the other proceeds at a finite rate, and the value of any extensive property for the system is a linear mole-fraction sum of its values for the individual phases.

The equations of motion are the one-dimensional Euler equations, which neglect viscosity and transport processes,

$$\dot{\rho} + \rho u_x = 0 \quad ,$$

$$\dot{u} + v p_x = 0 \quad ,$$

$$\dot{e} + p\dot{v} = 0 \quad ,$$

$$\dot{\lambda} = r \quad ,$$

and

$$\dot{f} \approx f_t + u f_x, \quad f = f(x,t) \quad . \tag{1}$$

Shocks are discontinuous jumps, and the only entropy-producing process other than the shock transition is the finite-rate phase transformation.

I. THE EQUATION OF STATE

We use a particularly simple equation of state for which p depends only on v and λ, and not on e (that is, the Gruneisen gamma is zero). In Sec. A we write down the EOS (equation of state) $p(v,\lambda)$. In Sec. B we consider a set of thermal properties consistent with this form and make the necessary assumptions to make λ_e, the equilibrium value of λ, independent of T. We make no further reference to T or e beyond this section. In Sec. C we discuss the equilibrium EOS $p(v)$. Finally, we give two illustrative numerical examples of the EOS in Sec. D.

A. The EOS $p(v,\lambda)$

We describe each pure phase by an EOS with p a function of v only.

$$p = \widetilde{p}_i(v_i) \text{ or } v_i = \widetilde{v}_i(p), \quad i = 1,2 \quad . \tag{2}$$

This of course implies that the isotherm, isentrope, Hugoniot, etc., all coincide in p-v space. In addition, we have additive volumes

$$v = (1 - \lambda)\widetilde{v}_1(p) + \lambda\widetilde{v}_2(p) \quad . \tag{3}$$

We further specialize to a γ-law form with $\gamma = 2$ for the pure-phase equations of state

$$\widetilde{p}_i(v_i) = p_0(v_{0i}/v_i)^2 \tag{4}$$

with

$$p_0 = 1, \ v_{01} = 1, \ v_{02} = kv_{01} \quad . \tag{5}$$

The dial k controls the amount of volume change. The mixed-phase EOS is then $\overline{p}(v,\lambda)$ or $\widetilde{v}(p,\lambda)$.

$$\overline{p}(v,\lambda) = (\overline{v}_0/v)^2 = (1 + \lambda q)^2/v^2 \quad ,$$

$$\overline{v}_0 = (1 - \lambda)v_{01} + v_{02} = 1 + \lambda\Delta v_0 = 1 + \lambda q \quad ,$$

and

$$q \equiv \Delta v_0 \approx v_{02} - v_{01} = (k - 1)v_{01} \quad . \tag{6}$$

We have used the symbol q, which usually denotes the heat of reaction, for Δv_0, the volume change at p_0, since it plays a similar role in the EOS.

Regarding p as a function of e, v, and λ the partial derivatives of interest are

$$-p_v = \rho^2 c^2 = 2p/v \quad ,$$

$$p_e = 0 \quad ,$$

$$p_\lambda = \rho c^2 \sigma = 2p \, \Delta v_0/\overline{v} \quad ,$$

and

$$c^2 = 2pv \propto p^{1/2} \quad . \tag{7}$$

Here c is the frozen sound speed, the isentropic derivative at constant λ, and σ is the Wood-Kirkwood effective-exothermicity coefficient which appears in the adiabatic-change relation or "master equation"

$$\dot{p} = c^2 \dot{\rho} + \rho c^2 \sigma \dot{\lambda} \quad . \tag{8}$$

B. Thermal Properties.

We discuss the thermal properties and the energy here mainly to determine the assumptions needed to get simple properties, such as a fixed transition pressure. We will make no reference to thermal properties beyond this section.

For each phase we choose the reference point (p_0, v_{0i}) on the EOS, and T_0, a reference value of T. We will ultimately refer the energy of each phase to its energy at (p_0, T_0, v_{0i}), which we denote by $\hat{e}_i$.

$$\hat{e}_i = e_i(p_0, T_0, v_{0i}) \quad . \tag{9}$$

We start by calculating the energy relative to that at $(p_0, T = 0, v_{0i})$.

$$e_i(p,T,v) = e_i(p_0,T=0,v_{0i}) - \int_{v_{0i}}^{v} \tilde{p}_i dv + I_c$$
$$I_c = \int_0^T C_i dT \quad . \tag{10}$$

The first integral is taken at constant temperature, $T = 0$, and the second at that constant volume which is the upper limit of the first. We assume that C_i is independent of volume and do not specify it in complete detail, but do take it to be constant above T_0. We may then write

$$e_i(p,T) = \hat{e}_i + p\tilde{v}_i(p) - p_0 v_{i0} + C_i(T - T_0)$$

and

$$\hat{e}_i = e_i(p_0,T=0,v_{0i}) + I_c \quad , \tag{11}$$

where we have evaluated the first integral in Eq. (9) from the EOS.

The Gibbs free energy g_i is

$$g_i(p,T) = e_i(p,T) - Ts_i(T) + p\tilde{v}_i(p) \quad ,$$

$$s_i(T) = C_i \ln T/T_0 + s_i \quad ,$$

and

$$s_i = s_i(p_0, T = 0, v_{0i}) + I_c \quad , \tag{12}$$

where s is entropy. Equating the Gibbs free energies of the two phases gives the phase line $p^*(T)$.

$$[p^*(T)/P_0]^{1/2} = (\Delta\hat{e} - T\Delta\hat{s} + \Delta CT \ln T/T_0)/p_0\Delta v_0) - 1 \quad . \tag{13}$$

To make things simple, we take the case of equal heat capacities and reference entropies, that is $\Delta C = \Delta\hat{s} = 0$, so that $p^*(T)$ is constant. We choose the value of p^* and let this determine $\Delta\hat{e}$, which turns out to be positive.

$$\Delta\hat{e}/(p_0\Delta v_0) = 1 + (p^*/p_0)^{1/2} \tag{14}$$

C. The Equilibrium EOS p(v)

The EOS $p(v,\lambda)$ is the one-parameter (λ) family of curves in the p-v plane shown in Fig. 1. The EOS is defined only in the region spanned by this family. Since the transition pressure p^* is constant by virtue of the assumptions of the preceding section, the equilibrium equation of state, the heavy line in the figure, takes a particularly simple form. It consists of (1) the portion of the $\lambda = 0$ curve above p^*, on which $\lambda_e = 0$; (2) the horizontal line segment between $\lambda = 0$ and $\lambda = 1$ at $p = p^*$, on which λ_e is given by the lever rule

$$\lambda_e = \lambda_e(v) = (v - v_1^*)/(v_2^* - v_1^*)$$

and

$$v_1^* = \tilde{v}(p^*,\lambda = 0), \quad v_2^* = \tilde{v}(p^*,\lambda = 1) \quad ; \tag{15}$$

and (3) the portion of the $\lambda = 1$ curve below p^*, on which $\lambda_e = 1$.

Point 0 at (p_0, v_{01}) is the metastable initial state for the detonations we will study. The metastable extension of the $\lambda = 0$ curve below p^* will be important to our discussion; the metastable portion of $\lambda = 1$ above p^* will not be used.

D. Numerical Examples

The equilibrium EOS plus the metastable extension of $\lambda = 0$ is given in Table I and Fig. 2 for two values of the volume ratio

$$k = 1.2 \text{ and } 1.4 \quad .$$

The values of u in Table I are for the equilibrium rarefaction wave discussed in Sec. V.

II. THE REACTION RATE

Although we will make no use of an explicit reaction rate in our discussion, we will want to occasionally refer to some of its general properties. For definiteness, we set down here a simple rate proposed by Duvall.* We first define a function $\lambda_e(v)$ which is the straightforward extension of the λ_e of Eq. (14) to the entire physical region of the p-v plane.

$$\widetilde{\lambda}_e(V) = 0 \quad , \qquad v < v_1^* \quad ;$$

$$\widetilde{\lambda}_e(v) = (v - v_1^*)/(v_2^* - v_1^*), \quad v_1^* \leq v \leq v_2^* \quad ;$$

and (16)

$$\widetilde{\lambda}_e(v) = 1 \quad , \qquad v > v_2^* \quad .$$

The rate function is then

$$r(v, \lambda) = \widetilde{\lambda}_e(v) - \lambda \quad . \tag{17}$$

Since the constant-λ curves have negative slope, the rate function is positive everywhere above p^* and negative everywhere below as shown in Fig. 3.

---

*Y. Horie and G. E. Duvall, "Shock-Induced Phase Transition in Iron," IUTAM Symposium on High Dynamic Pressure, 1967, pp. 355-359.

III. HYDRODYNAMICS: SOLUTION SEGMENTS

In this section we give equations for the pieces which are patched together to make up the rarefaction-wave and detonation-wave solutions of Secs. IV and V.

A. Rarefaction

For a forward-facing simple wave we have (at fixed composition, γ-law EOS)

$$u - 2c/(\gamma - 1) = \text{constant}$$

and

$$u + c = x/t \text{ (centered wave)} \quad . \tag{18}$$

For $\gamma = 2$ we have, eliminating c from the second equation,

$$u - 2c = \text{constant}$$

and

$$u = (2/3) x/t + \text{constant (centered wave)} \quad . \tag{19}$$

B. Detonation and Deflagration

We want to find (1) the final state of a steady detonation or deflagration given either (a) the final particle velocity u (overdriven wave) or (b) that the CJ condition applies (unsupported wave) and (2) the profile through the reaction zone, i.e., state as a function of degree of reaction λ through such a wave, given its propagation velocity D. Our notation will be (1) plain symbol = final state (end of reaction zone) and (2)^ = initial state. (Recall throughout that subscript 0 denotes EOS parameters, not in general the initial state for the wave.) We write our equations for $\hat{u} = 0$, so that velocities are relative to the initial state. (If $\hat{u} \neq 0$, replace u by u - $\hat{u}$ and D by D - $\hat{u}$.)

The equations to be solved all turn out to be cubics in v, which we represent as $f(v) = 0$. These are probably most easily solved by Newton-Raphson iteration.

4

TABLE I

EOS FOR VOLUME RATIOS k = 1.2 AND 1.4

$$(p_0 = 1, v_{01} = 1, v_{02} = kv_{01})$$

$$\lambda = 0 \ (\bar{v}_0 = 1)$$

p	v	c	u	u + c	ρc
9	0.3333	2.449	0	2.449	7.347
8	0.3535	2.378	-0.144	2.234	6.727
7	0.3779	2.300	-0.298	2.002	6.086
6	0.4082	2.213	-0.474	1.739	5.421
* 5	0.4472	2.115	-0.670	1.445	4.729
4	0.5000	2.000	-0.898	1.102	4.000
3	0.5774	1.861	-1.176	0.685	3.223
2	0.7071	1.682	-1.534	0.148	2.379
1.5	0.8165	1.565	-1.768	-0.203	1.917
1	1.0000	1.414	-2.070	-0.656	1.414

$$\lambda = 1, \ k = 1.2 \ (\bar{v}_0 = 1.2)$$

p	v	c	u	u + c	ρc
* 5	0.5367	2.317	---	---	4.317
4	0.6000	2.191	---	---	3.652
3	0.6928	2.039	---	---	3.238
r 2.88267	0.7068	2.019	-1.411	0.608	2.857
j 2.40369	0.7740	1.929	-1.591	0.338	2.492
2	0.8485	1.842	-1.765	0.077	2.171
1.5	0.9798	1.715	-2.019	-0.304	1.750
1	1.2000	1.549	-2.315	-0.766	1.29

$$\lambda = 1, \ k = 1.4 \ (v_{02} = 1.4)$$

p	v	c	u	u + c	ρc
* 5	0.6261	2.5022	---	---	3.996
4	0.7000	2.366	---	---	3.381
j 3.639111	0.7339	2.311	---	---	3.149
3	0.8083	2.202	---	---	2.725
r 2.51713	0.8824	2.108	-1.710	0.399	2.388
2	0.9899	1.990	-1.945	0.045	2.010
1.5	1.1431	1.851	-2.224	-0.373	1.620
1	1.4000	1.673	-2.978	-1.305	1.195

Notes:

1. The values of u are for the equilibrium centered rarefaction wave from $p/p_0 = 9$, $\lambda = 0$, u = 0 (Sec. IV). (Below $p/p_0 = p*/p_0 = 5$ the values on $\lambda = 0$ are for the frozen wave.)

2. The points marked *, r, and j are the transition point, the final state of the CJ deflagration (rarefaction shock) from $p = p*$, $\lambda = 0$; and the final state of a CJ detonation in metastable phase 1 ($\lambda = 0$) at $v = v_{01}$.

Equations

$$v = \bar{v}_0 \ (p/p_0)^{-1/2}; \quad \bar{v}_0 = (1-\lambda)v_{01} + \lambda v_{02} \ .$$

$$c = (2 \ pv)^{1/2} \ .$$

$$u = u_i + 2 \ (c-c_i) \ ,$$

where state i is $p = 9$, $\lambda = 0$ ahead of the rarefaction shock, and state r behind it.

5

$$v^{n+1} = v^n - f(v^n)/f'(v^n) \quad . \tag{20}$$

In each case we will sketch the form of the function $f(v)$ and comment on features affecting the iteration.

We draw all of our p-v figures in the context of the present example: the initial state for a detonation is our standard initial state, point 0 of Fig. 2a, and the initial state for a deflagration (here labeled N) is a shocked state like state A of the same figure.

1. Final State for Given u, Fig. 4a. The initial state will be 0 for a detonation and N for a deflagration; the final state for either is the strong point s.

Since u is given, we have

$$u^2 = (p - \hat{p})(\hat{v} - v) \quad . \tag{21}$$

Expressing p in terms of v by the EOS gives

$$f(v) = \hat{p}v^3 - (u^2 + \hat{p}\hat{v})v^2 - p_0\bar{v}_0^2 v + p_0\bar{v}_0^2\hat{v} = 0$$

and

$$f'(v) = 3\hat{p}v^2 - 2(u^2 + \widehat{pv}) - p_0\bar{v}_0^2 \quad , \tag{22}$$

where $\bar{v}_0(\lambda)$ is to be evaluated at the final λ. The desired strong root is at the left; convergence to it is guaranteed by taking the initial guess for v at the inflection point $f''(v) = 0$.

2. Final State Given the CJ Condition, Fig. 4b. Again the initial state will be 0 for a detonation and N for a deflagration. In the figure as drawn the final state j is the same for both. The dashed Rayleigh lines for each case go to the solution which is **not** desired.

The CJ condition results in the tangency requirement

$$(\partial p/\partial v)_\lambda = (p - \hat{p})/(v - \hat{v}) \quad , \tag{23}$$

with the derivative on the left to be evaluated on the final-λ locus. For our EOS, $(\partial p/\partial v)_\lambda = -2p/v$. Using this and the EOS for p we find

$$f(v) = \hat{p}v^3 - 3p_0\bar{v}_0^2 v + 2 p_0\bar{v}_0^2\hat{v} = 0$$

and

$$f'(v) = 3\hat{p}v^2 - 3p_0\bar{v}_0^2 \quad . \tag{24}$$

This time f(v) has no inflection point and convergence to the desired root is guaranteed by starting at the initial volume $\hat{v}$ in either case.

3. Steady Solution for Given D, Fig. 4c. The initial state is point N for the deflagration and point 0 for the detonation (although of course N would do equally well for it also). We want the strong branch of the solution in either case.

Since the solution must lie on the Rayleigh line we have

$$(\widehat{\rho D})^2 = (p - p)/(\hat{v} - v) \quad . \tag{25}$$

Using the EOS for p gives

$$f(v;\lambda) = (\widehat{\rho D})^2 v^3 - [\hat{p} + (\widehat{\rho D})^2\hat{v}]v^2 + p_0[\bar{v}_0(\lambda)]^2 = 0$$

and

$$f_v = 3(\hat{\rho D})^2 v^2 - 2[\hat{p} + (\widehat{\rho D})^2\hat{v}]v \quad . \tag{26}$$

Again we are bothered by an inflection point; we can guarantee convergence to S by starting the iteration at the inflection point $f_{vv}(v;\lambda) = 0$. Note that if we can use the solution in the form $\lambda(v)$ instead of $v(\lambda)$, that is, if we have found the end points and are willing to pick values of v instead of λ, then we have a simple explicit solution, using $\bar{v}_0 = v_{01} + \lambda q$.

$$(v_{01} + \lambda q)^2 = \{-\widehat{\rho D}^2 v^3 + [\hat{p} + (\widehat{\rho D})^2\hat{v}]\}/p_0 \quad . \tag{27}$$

The slope of $v(\lambda)$ or $p(\lambda)$ is positive and finite throughout except in the CJ case where it goes to infinity in the final state.

IV. THE RAREFACTION WAVE

We consider a centered rarefaction wave beginning in an equilibrium state above the transition pressure on the $\lambda = 0$ locus, such as point I of Fig. 2a. The wave is approximately self-similar so that a plot of state against x/t is appropriate. In this plot a

feature of fixed physical width, such as the deflagration wave which appears at late times, shrinks to zero width as t → ∞; we may thus speak of it as a rarefaction shock. The time scale is the reaction time; "early" or "late" refers to times small or large compared to the reaction time.

At sufficiently early time we have just the frozen rarefaction wave, lying completely on the $\lambda = 0$ branch of the EOS. At sufficiently late time we have the configuration implied by the equilibrium EOS, with some type of transition from $\lambda = 0$ to $\lambda = 1$ at $p = p^* = 5$. Table I includes values of ρc and $u + c$; these and other quantities are sketched in Fig. 5 for the equilibrium EOS. With these in mind, we now consider the limiting late-time waveform implied by the equilibrium EOS, temporarily ignoring the finite reaction rate.

The form of the equilibrium EOS implies the existence of a rarefaction shock within the wave. We digress briefly here to insert the more-or-less standard discussion of this phenomenon.* Consider the bumpy p-v isentrope of Fig. 6. The tangent points 1 and 2 will be connected by a rarefaction shock. Let ξ be the material coordinate defined as the particle position in a reference configuration of uniform density $\hat{\rho}$. The characteristic and shock speeds are

$$(d\xi/dt)_{char} = -\rho c/\hat{\rho} = -[(\partial p/\partial v)/\hat{\rho}]^{1/2}$$

and

$$(d\xi/dt)_{shock} = -([p]/[v])^{1/2} , \qquad (28)$$

where the square brackets denote the jump across the shock. The characteristic speeds at points 1 and 2 and the speed of the rarefaction shock joining them are all equal. In a noncentered rarefaction wave, the characteristics from points between 1 and 2 would cross to form a rarefaction shock, which would grow in strength until it extends from point 1 to point 2. The characteristic diagram for a centered wave with rarefaction shock is shown in Fig. 6b.

Now suppose that we support the rarefaction shock by applying a rear boundary condition of constant p or u greater than that of the terminal state 2. We will then get a rarefaction shock like 1'-2'. This supported rarefaction shock is weaker and runs

_____

*This seems to be common knowledge, but I do not have a reference at hand.

slower and is overtaken by characteristics coming from the constant state behind, as shown in Fig. 6c.

Figures 7 and 8 give calculated results for the centered rarefaction wave from $p = 9$, $\lambda = 0$ in the $k = 1.2$ material. Figure 7 shows the principal characteristics in t-h and t-x ($h = \hat{\rho}\xi$) for the equilibrium ($t = \infty$) wave, and Fig. 8 shows the pressure profiles for both the frozen ($t = 0$) and equilibrium ($t = \infty$) waves.

The equilibrium wave consists of, from front to back,

(1) A conventional rarefaction wave at $\lambda = 0$ from points I to A, Fig. 2;

(2) A constant-state region which "turns the corner" at A;

(3) The rarefaction shock A-r, through which the composition jumps instantaneously from $\lambda = 0$ to $\lambda = 1$; and

(4) A conventional rarefaction at $\lambda = 1$ from r on down.

The "rarefaction shock" is of course actually a steady CJ deflagration wave of finite width, with a structure like that of the steady detonation reaction-zone discussed in the next section. Recall the discussion at the beginning of this section.

V. THE DETONATION WAVE

We now consider steady detonation waves (in metastable phase 1 at v_{01}) supported by a piston of specified constant velocity u_p.

We take up the simplest case first: piston velocities corresponding to shocks from point 0 to points on $\lambda = 0$ above the transition pressure. In Fig. 9, these are shocks to points on $\lambda = 0$ above point A, that is, for $u_p \geq u_A$, where u_A is the particle velocity produced by a shock to point A. For all such u_p the shocked state is on the equilibrium branch of $\lambda = 0$, so that the (instantaneous) shock jump produces no reaction at all, and all such waves are just nonreactive shocks.

For lower piston velocities we must distinguish two cases depending on the size of the volume ratio k. The two materials of Table I and Fig. 2, with k = 1.2 and k = 1.4, furnish an example of each. The behavior depends on whether k is greater or less

than the critical value $\tilde{k}$ at which points j and r coincide. For $k < \tilde{k}$ point r, Fig. 9, is above point j and *vice versa* for $k > \tilde{k}$.

In the following discussion we will be dealing with quasi-steady double-wave structures, with the two waves moving at different velocities. It must of course be remembered that in this case the point on the equilibrium locus picked out by specifying the final particle velocity is not the same as the usual one for a single steady wave, that is, the point on the equilibrium locus which satisfies

$$u_p^2 = (p - 1)(1 - v) \quad . \tag{29}$$

Instead, the final particle is that behind the second wave.

A. Case 1: $k < \tilde{k}$

We consider the unsupported case first. For small enough u_p we have just the conventional CJ detonation consisting of a nonreactive shock to point A', Fig. 9, on the metastable branch of $\lambda = 0$, followed immediately by a steady reaction zone (deflagration) which moves the state point down the Rayleigh line from A' to the CJ point j on the equilibrium branch of $\lambda = 1$. The pressure and volume as a function of degree of reaction λ, as given by Eq. (25), are plotted in Fig. 10. This solution remains as u_p is increased, until u_p becomes greater than u_j, the CJ particle velocity at the end of the reaction zone.

As the piston velocity is further increased, we have the conventional overdriven detonations until the lead shock point reaches the transition pressure at A, that is for $u_j < u_p \leq u_B$, Fig. 9.

For larger piston velocities $u_B < u_p \leq u_A$ we have a double-wave structure. The lead shock is still the shock to point A, as for $u_p = u_B$, but the fire now lies along a less steep Rayleigh line like OC and is decoupled from the shock since it runs slower. Thus we have a double-wave structure with an increasing zone of constant state ($p = p^*$, $\lambda = 0$) separating the start of the fire (head of the deflagration wave) from the shock. The state C at the end of the fire is of course still subsonic. Both the pressure jump across the fire and the fire velocity decrease with increasing u_p, becoming zero at $u_p = u_A$.

B. Case 2: $k > \tilde{k}$

The conventional CJ detonation no longer exists, for its initial shocked state A', Fig. 2b, lies on the stable branch of $\lambda = 0$ and is thus an equilibrium state, so that no reaction occurs. The unsupported detonation for $u_p \leq u_r$ is a double wave like that of case 1 for $u_B < u_p < u_A$: The shocked state is point A, and the fire, which is the CJ deflagration from this shocked state to the tangent point r on (the stable branch of) $\lambda = 1$, runs slower than the lead shock. However, the final state j is now sonic. for piston velocities above u_r, $u_r < u_p \leq u_A$, the lead shock is unchanged, but again both the pressure jump across the fire and the fire velocity decrease as u_p increases and vanish at $u_p = u_A$.

We remark that in case 1, for a detonation with initial shock to point A the CJ fire velocity is greater than the shock velocity (the CJ fire Rayleigh line A-r is steeper than the CJ detonation Rayleigh line A-O, Fig. 9). If a wave were set up with shock to A followed by the fire at some distance behind the shock, the fire would overtake the shock and degrade it down to the CJ detonation.

In Part A we considered steady inviscid solutions; here we study the same system but allow viscosity. Our primary interest is the inviscid limit. For lack of time we limit ourselves to a preliminary qualitative discussion of the main features. For background, see Fickett and Davis,[*] Sec. 5F. We will call the solution described there the *conventional solution.*

I. EQUATIONS

The equations are the same as those of the inviscid case with the pressure p replaced by the sum of the hydrostatic pressure and the normal viscous stress π.

$$\pi = - \nu u_x \quad , \tag{30}$$

with ν the viscosity coefficient. Because of our simple EOS, we do not need the energy equation. Our equations are, then, (in the steady frame)

$$\rho u = m \text{ or } u = mv, \ m \equiv \rho_0 D \quad ;$$

$$\pi + p - p_0 = m^2(v_0 - v) \quad ;$$

and

$$d\lambda/dx = z\widetilde{r}/mv \quad , \tag{31}$$

where m is the constant mass flux. We have expressed the rate r as $z\widetilde{r}$, to make the multiplier z explicit. Using the EOS we can write these equations as

$$\ell_v \ dv/dx = R(v,\lambda,m) \quad , \tag{32a}$$

$$\ell_r \ d\lambda/dx = \widetilde{r}(v,\lambda)/(v/v_0) \quad , \tag{32b}$$

$$R(v,\lambda;m) = (p - p_0)/m^2 - v_0 - v) \quad ,$$

$$= [\hat{p}\hat{v}_1{}^2 \ (1 + q\lambda)^2 - p_0]/m^2 - (v_0 - v) \quad ,$$

_____
[*]W. Fickett and W. C. Davis, *Detonation,* a LASL monograph. To be published.

and

$$\ell_v = v/m, \ \ell_r = m/\rho_0 z = D/z \quad , \tag{33}$$

where ℓ_v and ℓ_r are characteristic viscous and reaction lengths, and the "Rayleigh function" R is zero on the Rayleigh line and positive for higher pressures. An example of $\widetilde{r}$ would be the rate expression given by Eq. (16). There is then a single ordinary differential equation for the desired steady solution $v(\lambda)$

$$\epsilon dv/d\lambda = vR(v,\lambda;m)/r(v,\lambda);$$
$$\epsilon = \ell_v\ell_r = z\nu/\rho_0 \ D^2 \quad . \tag{34}$$

(Eq. 32b then gives the x-dependence.) Note that for a given substance and initial state both R and ϵ depend on the wave velocity D. The boundary conditions are the same as those for the inviscid case plus the requirement that the gradients (in x) vanish at x $= \pm \infty$. To get a steady solution with metastable initial state we must impose an "ignition limit," say

$$r = 0 \text{ for } v > \hat{v} \quad . \tag{35}$$

The parameter ϵ, the ratio of characteristic lengths, is not necessarily small, but we use this symbol because of our interest in the inviscid limit $\epsilon \to 0$.

II. THE PHASE PLANE

Figure 11 shows the complete phase-plane and corresponding p-v diagram. The main differences from the conventional case are:

(1) The Rayleigh line R = 0 can intersect the Hugoniot in as many as four points, and

2. The reaction is reversible, with portions of the r = 0 equilibrium locus lying in the interior and on the left boundary.

The integral curves are horizontal on R = 0 and vertical on r = 0. An example of the upper branch of R = 0 was given in Fig. 10; r = 0 is of course just p = p*, the equilibrium locus of Fig. 2.

The loci of constant pressure are hyperbolae with $v = 0$ at $\lambda = -1/q$ and with asymptotic slope inversely proportional to p,

$$v^2 = (1 + \lambda q)^2/p \quad , \tag{36}$$

the equilibrium locus $r = 0$ ($p = p^*$) being an example. The p-v and v-λ diagrams are of course topologically equivalent. The *turning* loci are $r = 0$ and $R = 0$; integral curves are vertical on $r = 0$ and horizontal on $R = 0$ (except of course at their intersections, the critical points). The signs of R and r are shown adjacent to the turning loci; from these are deduced the slopes of the integral curves in the various regions. Away from the turning loci the magnitude of the slope of the integral curves is inversely proportional to ϵ. The locus $r = 0$ is independent of D, but $R = 0$ is not: as D decreases, $R = 0$ shrinks and the extremum in λ moves to the left, and for small enough D, $R = 0$ intersects neither $r = 0$ nor $\lambda = 1$ and all of the critical points disappear.

Of the conventional critical points S' and W', S' is a mode and W' a saddle; we will need to consider only S' here. Of the new critical points S is a mode and W is a saddle. The separatrix so marked in Fig. 11 is of special importance. It is the particular integral curve going into point W from above; it separates the integral curves going to S from those going to W. The important questions (when W is present) are:

(1) Does the separatrix coming into W from above intersect $\lambda = 0$ above or below the ignition volume $\hat{v}$?

(2) Is S' present or absent?

Before proceeding to the discussion of possible steady solutions in the next section, we review the connection to the inviscid solution. In the inviscid case a shock is a jump from O to S on $\lambda = 0$. With viscosity but without reaction (λ fixed at 0), a shock is the solution of Eq. (32a), lying entirely on $\lambda = 0$ and extending from O to S. With small rate, this solution is bowed slightly inward to nonzero λ, but retains its end points as shown.

III. STEADY SOLUTIONS (D-DISCUSSION)

The key to the problem is the eigenvalue solution; we discuss it first. The discussion is essentially the same whether we fix the substance and vary D or fix D and vary the substance (that is, change the ratio ν/z); the important change in the equations is the value of ϵ in either case. We choose to fix D and vary the substance since then the Rayleigh line is unaffected by the variation and the pictures are less cluttered.

Let us start with a value of ϵ like that for which Fig. 11 is drawn, with the separatrix passing upwards to the right of the ignition point I. Consider Fig. 12. As ϵ is increased, the slope of the separatrix, like the slopes of all integral curves inside $R = 0$, decreases until at some particular value of ϵ, say $\tilde{\epsilon}$, the separatrix passes through point I. This is the *eigenvalue solution*. For $\epsilon = \tilde{\epsilon}$ the solution is the separatrix, and terminates in point W. For $\epsilon > \tilde{\epsilon}$ the separatrix (dashed line in the figure) intersects $\lambda = 0$ below $\hat{v}$ and the solution lies to its right and terminates at point S'. For $\epsilon < \tilde{\epsilon}$ the separatrix intersects $\lambda = 0$ above point I and the solution lies to its left and terminates in point S. Thus an infinitesimal change in ϵ across $\tilde{\epsilon}$ produces a large discontinuous change in the final state. The same solutions in p-v are also shown in Fig. 12.

Were we to fix the substance and vary D we would have essentially the same situation. At the eigenvalue velocity $\tilde{D}$ the solution goes to W; for larger D it goes to S (on the correspondingly slightly higher Rayleigh line) and for smaller D it goes to S'.

We are now ready to discuss the piston problem. We will not do this in complete detail but just indicate how it goes, with reference to the inviscid discussion already given in I. We will call the solutions just discussed the *upper* solution (to S), the eigenvalue solution (to W), and the *lower* solution (to S').

For large u_p, we have the upper solution. As we reduce u_p, D decreases until the eigenvalue velocity $\tilde{D}$ is reached. For u_p slightly below this, we have a two-wave structure: the first wave is the eigenvalue detonation to point W, and the second is a slower moving detonation from point W to point $\hat{S}$ on $\lambda = 0$ below S, which matches the prescribed piston velocity. This second wave is the left branch of the special solution of the critical point W, on a diagram for smaller D, Fig. 13. As the piston velocity is further reduced, the strength of the second wave is finally reduced to zero. On further reduction of u_p, we have for the second wave the deflagration from W to $\hat{S}'$, Fig. 13, the opposite branch of the special

solution of critical point W. (Note that the change in final volume with ϵ is discontinuous here but that the changes in p and u are not.) This branch W-$\hat{S}'$ is of course essentially the same as the following deflagration wave of the inviscid wave. As u_p is further reduced it gets stronger and moves faster until finally we have the truly steady single-wave solution O-W-S' of Fig. 12. Thus this range of quasi-steady two-wave solutions fills the gap between D infinitesimally greater than to infinitesimally less than $\tilde{D}$.

For smaller piston velocities we have the lower solution—the conventional blunted-spike over-driven detonation O-S'. From here on the conventional discussion applies.

We have taken the case analagous to $k < \tilde{k}$ of I. The lower solutions for the case analagous to $k > \tilde{k}$ are similar to those of I.

IV. THE INVISCID LIMIT

The inviscid limit is smoothly approached. As ϵ decreases to zero, points S and W go to point A, and $\tilde{D}$ approaches point D_A (Fig. 12, p-v). Point S' moves down along $\lambda = 1$. Thus the range of u_p over which the upper solution consists of two waves vanishes, and the corresponding range for the lower solution increases.

ACKNOWLEDGMENT
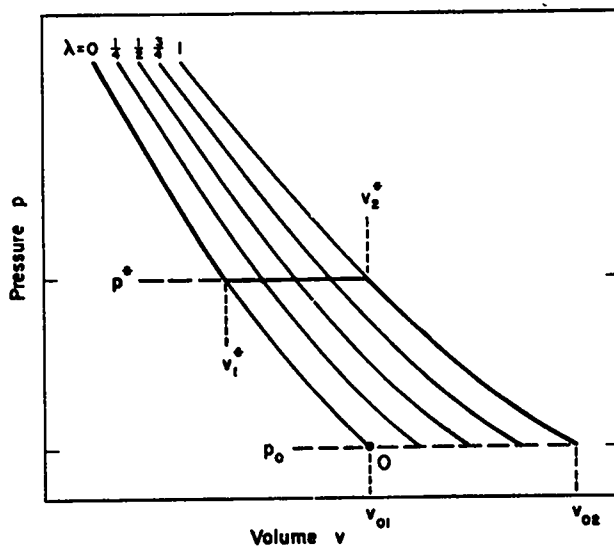
Fig. 1.
The EOS in p-v. The light lines show several
members of the one-parameter family p(v,λ) at
fixed λ; the heavy line is the equilibrium EOS
p(v).
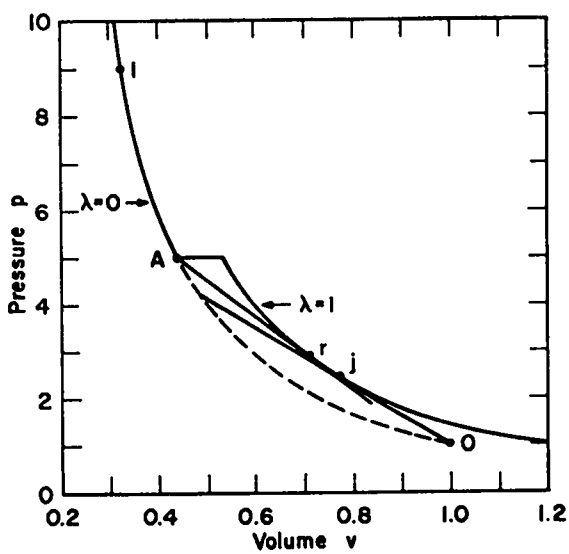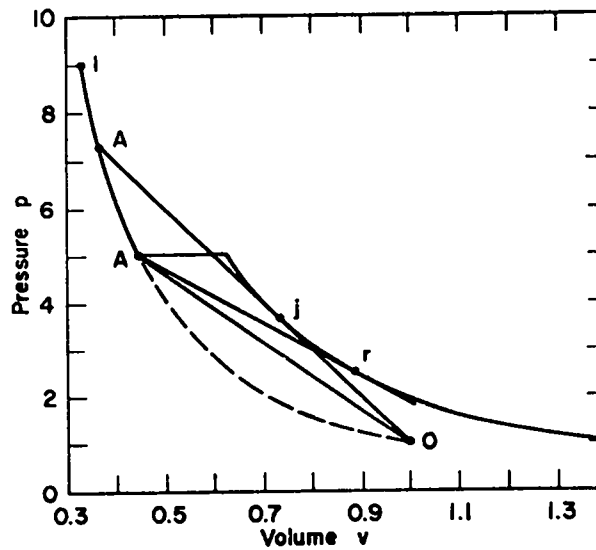
(a)   *(b)*

Fig. 2.
EOS for (a) k = 1.2, (b) k = 1.4.
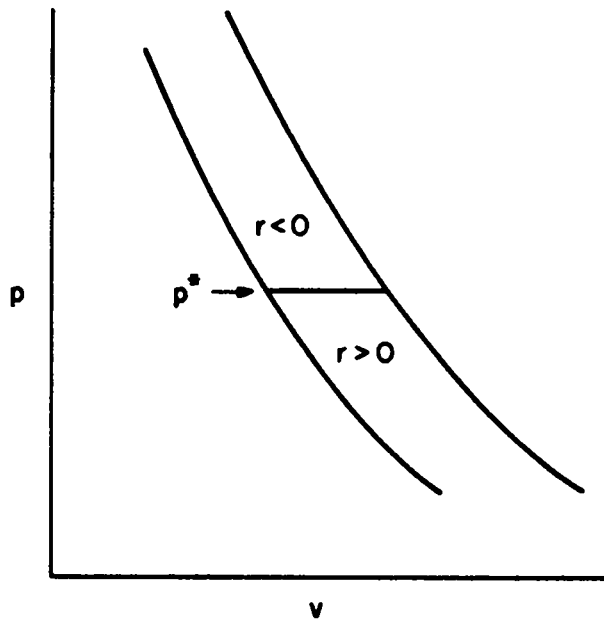
Fig. 3.
The sign of the rate function.
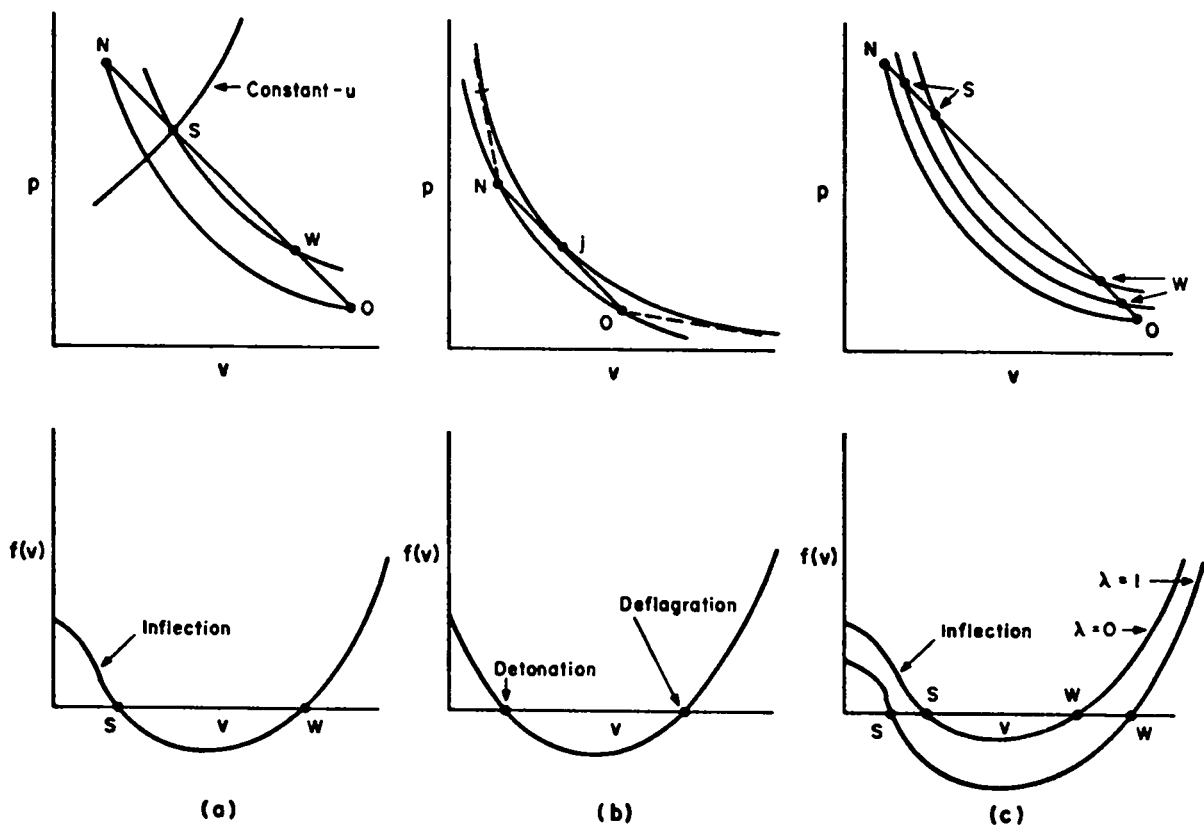
Fig. 4.
Steady deflagration and detonation solutions. (a) Final state for given u (overdriven). (b)
Final state given the CJ condition. (c) Complete solution given D. At CJ, λ = 1 is tangent.
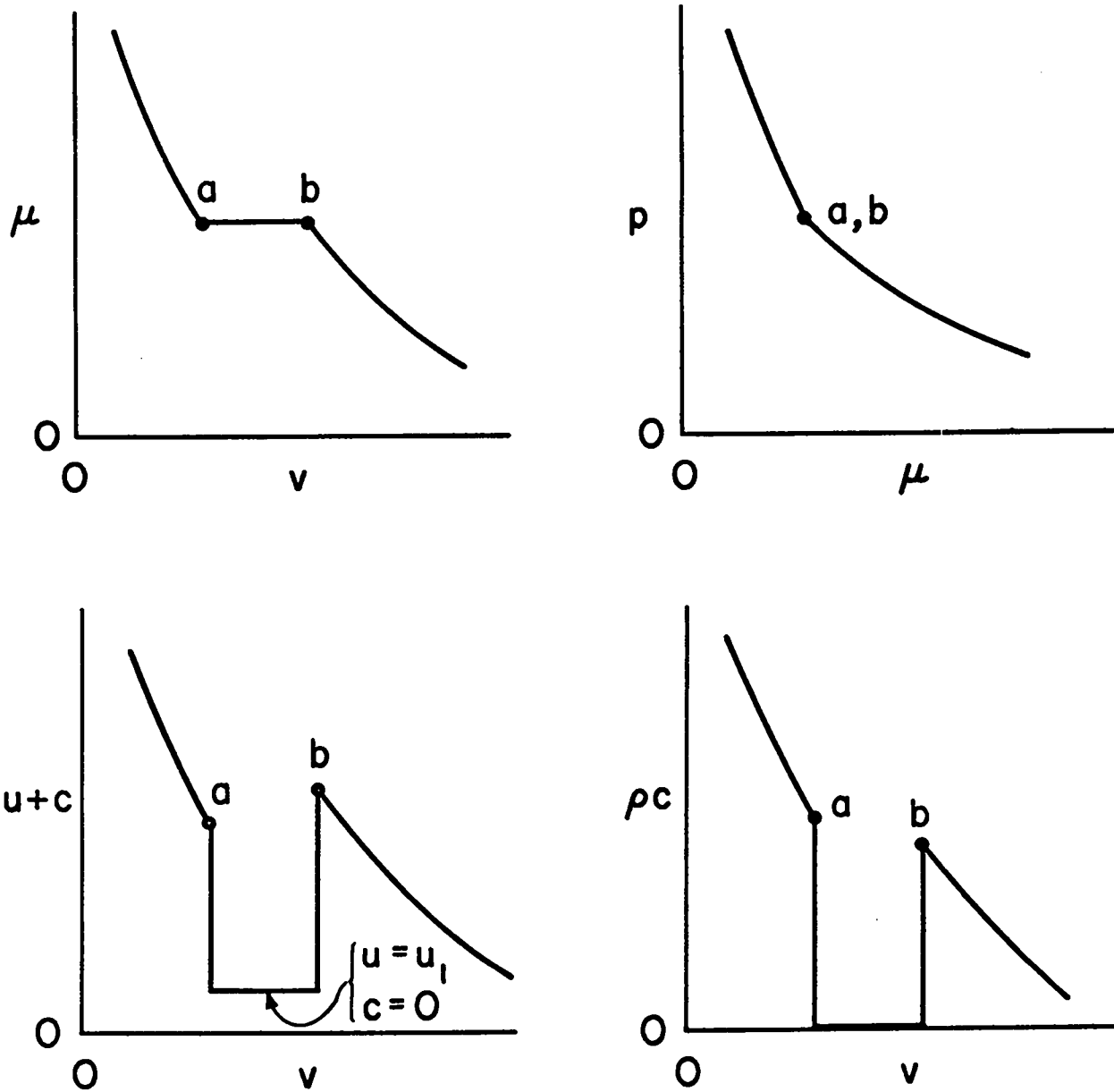
Fig. 5.
Sketch of various quantities through the equilibrium rarefaction wave.
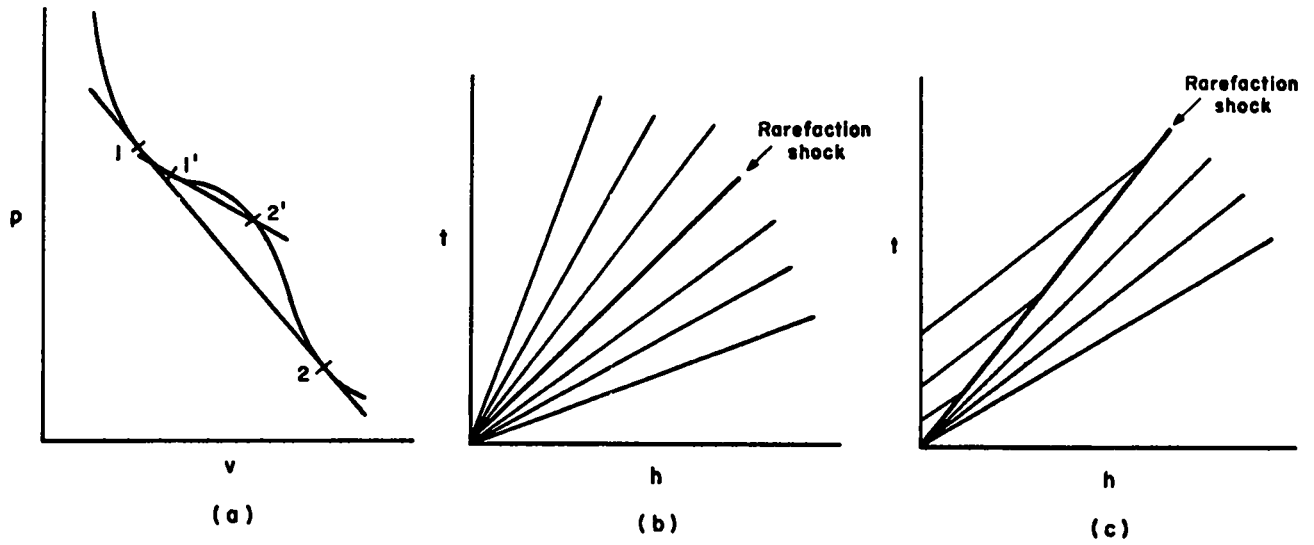
Fig. 6.

The rarefaction shock. (a) p-v diagram; (b) t-h diagram (h = ρ̂ξ) for the unsupported rarefaction shock 1-2; (c) same for the supported rarefaction shock 1'-2'.
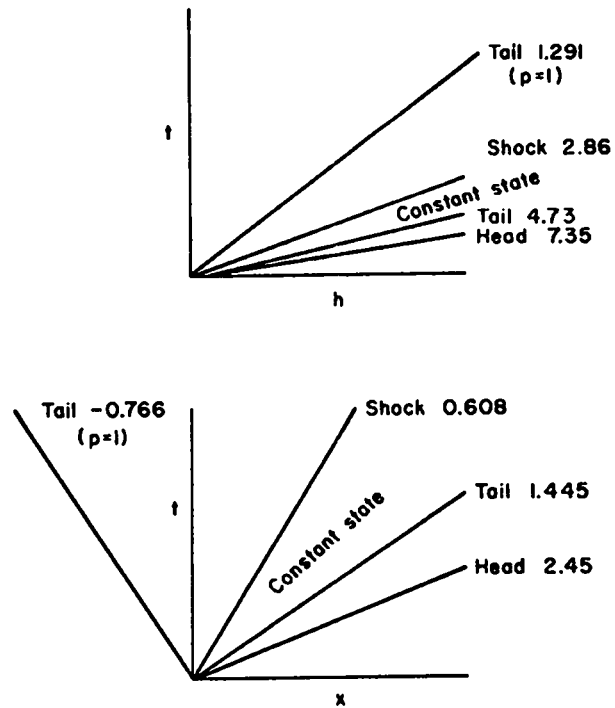
Fig. 7.

The t-h and t-x diagrams of the equilibrium rarefaction wave for k = 1.2. The numbers are the wave speeds.
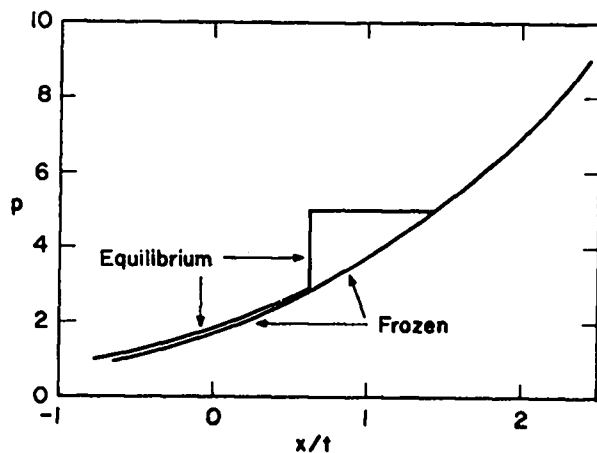
Fig. 8.
The frozen (t = 0) and equilibrium (t = ∞)
centered rarefaction waves for k = 1.2.
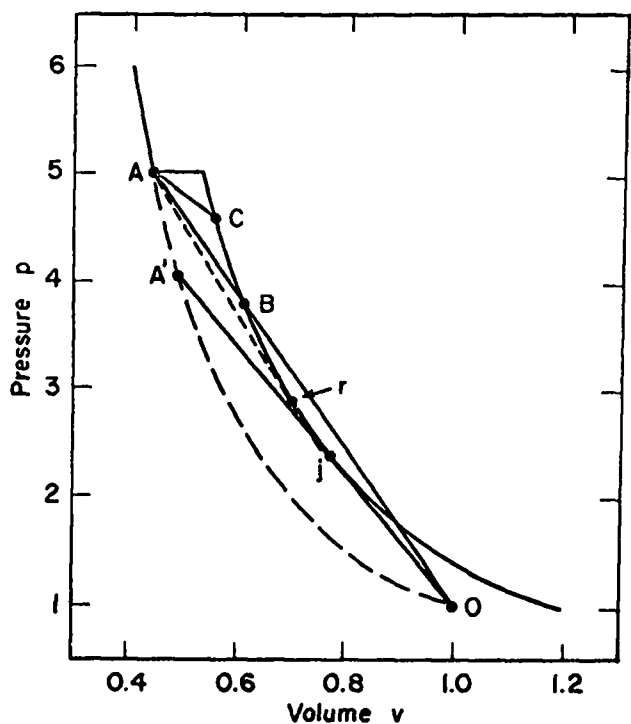
Fig. 9.
Magnified view of the lower portion of Fig. 2a,
showing different detonations for case 1, k<k̃
(k = 1.2).
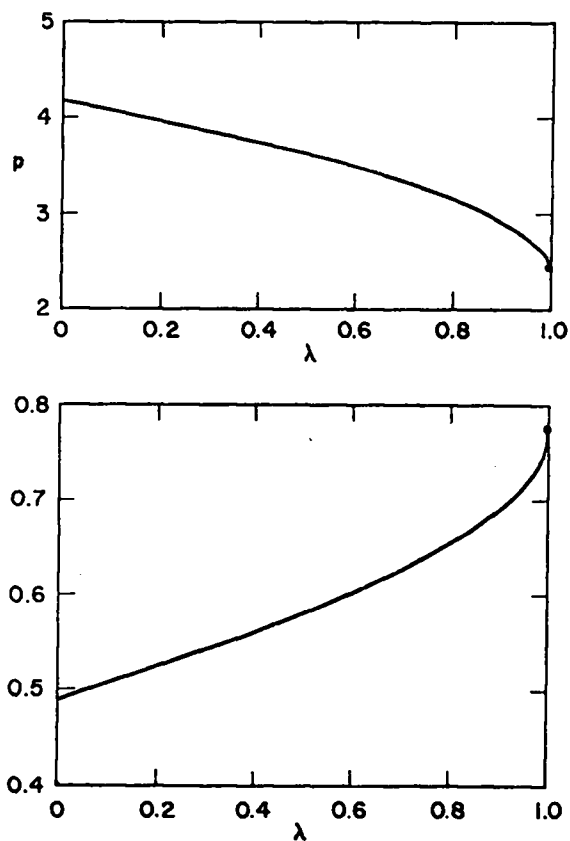
Fig. 10.
The steady CJ detonation reaction zone for
k = 1.2 (segment A'−j, Fig. 9); Dⱼ = 2.4922,
pᵢ = 2.5528.
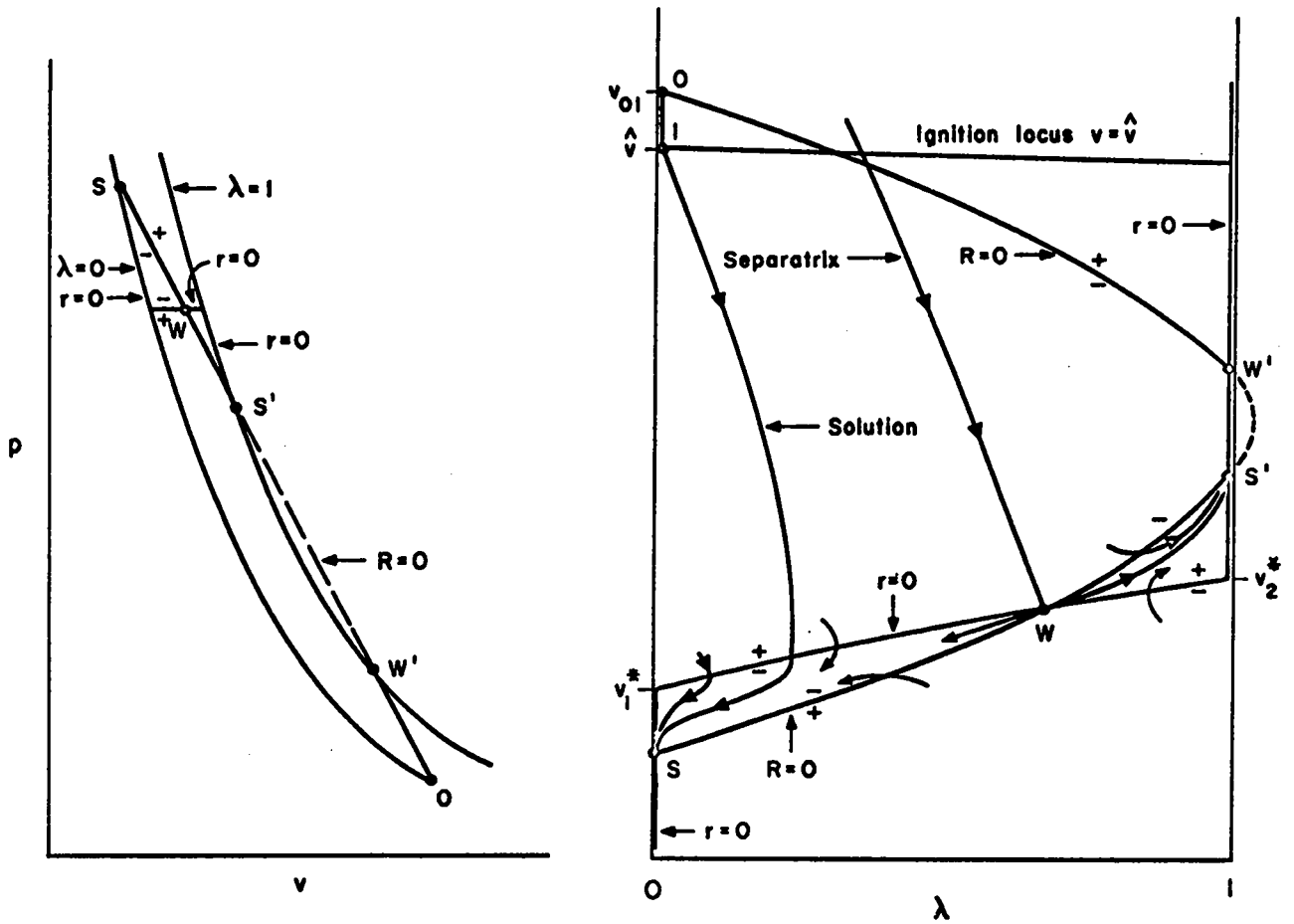
Fig. 11.
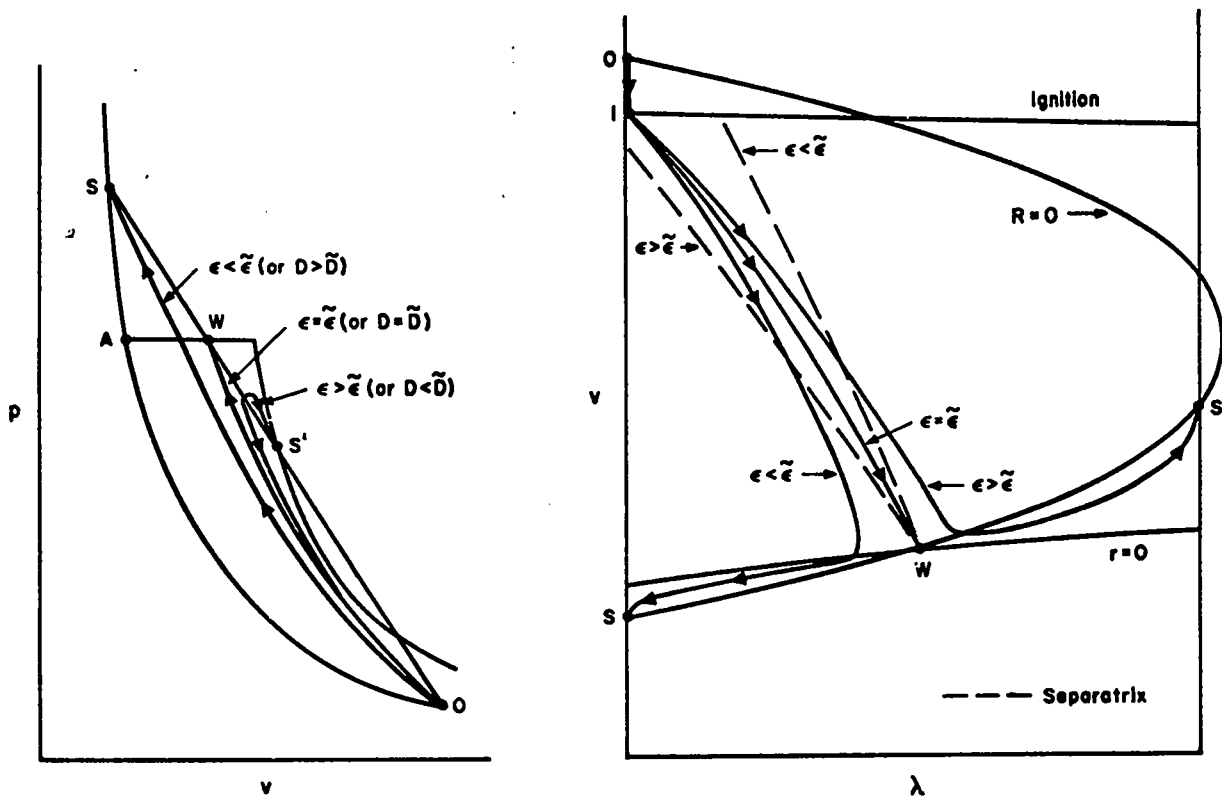*The p-v diagram and v-λ phase plane.*
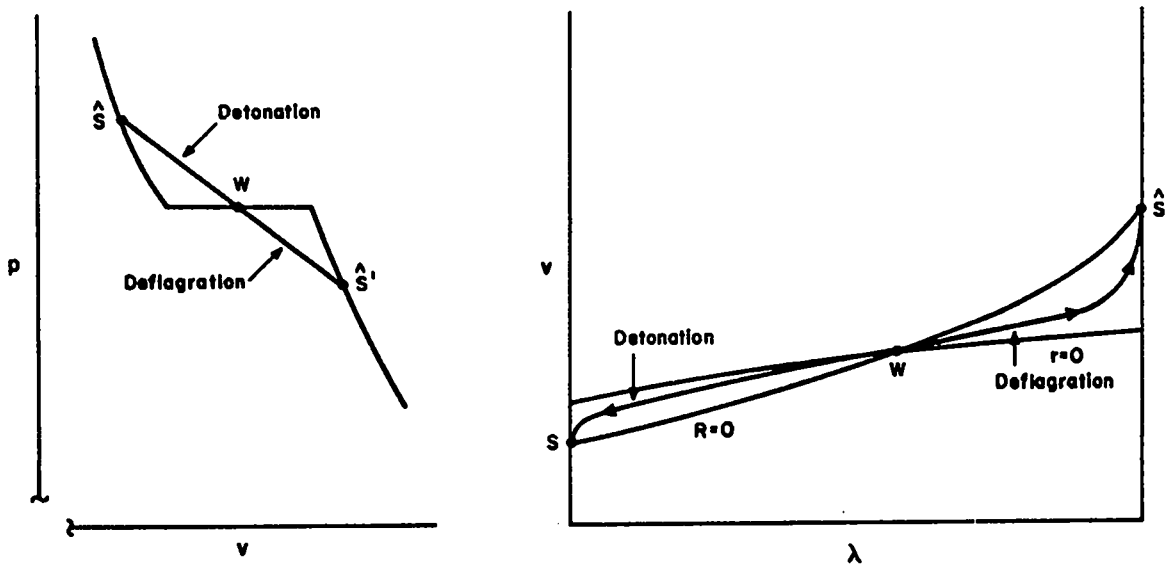
Fig. 12.
The eigenvalue detonation.

Fig. 13.
The slower second wave of the two-wave solution, from the eigenvalue state W at the end of the first wave.